ISSN 1674-1056
http://cpb.iphy.ac.cn
http://iopscience.iop.org/cpb
中国物理 B
Chinese Physics
中国物理
Chinese Physics B

Structures and local ferroelectric polarization switching properties of orthorhombic $YFeO_3$ thin film prepared by a sol-gel method

Runlan Zhang(张润兰), Shuaishuai Li(李帅帅), Changle Chen(陈长乐), Li-An Han(韩立安), Shanxin Xiong(熊善新)

Citation: Chin. Phys. B . 2019, 28(3): 037701. **doi:** 10.1088/1674-1056/28/3/037701
Journal homepage: http://cpb.iphy.ac.cn; http://iopscience.iop.org/cpb

What follows is a list of articles you may be interested in

Enhanced magneto-electric effect in manganite tricolor superlattice with artificially broken symmetry

Huanyu Pei(裴环宇), Shujin Guo(郭蜀晋), Hong Yan(闫虹), Changle Chen(陈长乐), Bingcheng Luo(罗炳成), Kexin Jin(金克新)

Chin. Phys. B . 2018, 27(9): 097701. **doi:** 10.1088/1674-1056/27/9/097701

Nanoscale domain switching mechanism of $Bi_{3.15}Eu_{0.85}Ti_3O_{12}$ thin film under the different mechanical forces

Zhu Zhe, Chen Yu-Bo, Zheng Xue-Jun

Chin. Phys. B . 2015, 24(10): 107702. **doi:** 10.1088/1674-1056/24/10/107702

Ferroelectricity in hexagonal $YFeO_3$ film at room temperature

Zhang Run-Lan, Chen Chang-Le, Zhang Yun-Jie, Xing Hui, Dong Xiang-Lei, Jin Ke-Xin

Chin. Phys. B . 2015, 24(1): 017701. **doi:** 10.1088/1674-1056/24/1/017701

Bipolar resistive switching in $BiFe_{0.95}Zn_{0.05}O_3$ films

Yuan Xue-Yong, Luo Li-Rong, Wu Di, Xu Qing-Yu

Chin. Phys. B . 2013, 22(10): 107702. **doi:** 10.1088/1674-1056/22/10/107702

Dielectric loss of half-doped manganite $La_{0.5}Ca_{0.5}MnO_3$

Cao Xian-Sheng, Ji Gao-Feng, Luo Bing-Cheng, Li Feng

Chin. Phys. B . 2013, 22(8): 087702. **doi:** 10.1088/1674-1056/22/8/087702

Structures and local ferroelectric polarization switching properties of orthorhombic $YFeO_3$ thin film prepared by a sol–gel method*

Runlan Zhang(张润兰)[1,†], Shuaishuai Li(李帅帅)[1], Changle Chen(陈长乐)[2], Li-An Han(韩立安)[3], and Shanxin Xiong(熊善新)[1]

[1] College of Chemistry and Chemical Engineering, Xi'an University of Science and Technology, Xi'an 710054, China
[2] Shaanxi Key Laboratory of Condensed Matter Structures and Properties, Northwestern Polytechnical University, Xi'an 710072, China
[3] College of Science, Xi'an University of Science and Technology, Xi'an 710054, China

(Received 12 September 2018; revised manuscript received 26 November 2018; published online 22 February 2019)

Orthorhombic $YFeO_3$ thin film was prepared on $La_{0.67}Sr_{0.33}MnO_3/LaAlO_3$ substrate by a sol–gel spin-coating method. The structures of the $YFeO_3/La_{0.67}Sr_{0.33}MnO_3/LaAlO_3$ (YFO/LSMO/LAO) sample were detected by x-ray diffraction pattern, Raman spectrometer, scanning electron microscopy, and atomic force microscope. The local ferroelectric polarization switching properties of the orthorhombic YFO film were confirmed by piezoresponse force microscopy (PFM) for the first time. The results show that the YFO film deposited on LSMO/LAO possesses orthorhombic structure, with ultra-fine crystal grains and flat surface. The leakage current of the YFO film is 8.39×10^{-4} A·cm^{-2} at 2 V, with its leakage mechanism found to be an ohmic behavior. PFM measurements indicate that the YFO film reveals weak ferroelectricity at room temperature and the local switching behavior of ferroelectric domains has been identified. By local poling experiment, polarization reversal in the orthorhombic YFO film at room temperature was further observed.

Keywords: multiferroics, $YFeO_3$ thin film, orthorhombic structure, piezoresponse force microscopy

PACS: 77.55.Nv, 77.84.–s, 68.37.Ps **DOI:** 10.1088/1674-1056/28/3/037701

1. Introduction

Multiferroics providing both ferroelectric and ferromagnetic (or antiferromagnetic) properties are well known for their intriguing physical origin and potential applications in sensor, actuation, and ferroelectric memory.[1–3] Meanwhile, they are promising materials in multiple-state memories, electric-field-controlled ferromagnetic resonance devices, and transducers with magnetically modulated piezoelectricity due to the magnetoelectric effect.[4–6] However, this kind of material is very rare as its two contrasting order parameters of ferroelectricity and magnetism turn out to be mutually exclusive.[4] Therefore, seeking new functional materials having multiferroic properties and exploring physical mechanism have been hot topics in the field of physics and material sciences.

Recently, RFeO$_3$ system was considered as a new type of multiferroics, regardless of the orthorhombic perovskite structure[7,8] or the hexagonal structure.[9,10] Orthoferrites (RFeO$_3$ with an orthorhombic perovskite structure) have been studied on the good magnetic, optical, and thermal properties for decades. There was hardly any report on the electric properties until the existence of ferroelectricity in the orthoferrites was testified. As a member of RFeO$_3$ system, $YFeO_3$ presents an orthorhombically distorted perovskite structure, with the iron ion surrounded by six oxygen atoms forming an octahedron. The presence of a Dzyaloshinskii–Moriya (DM) interaction can lead to a canting of the spin-lattice, resulting a weak ferromagnetic ordering in $YFeO_3$.[11] It is confirmed that $YFeO_3$ displays a transition from antiferromagnetic to paramagnetic at 655 K.[11] Although recent reports have shown the possibility of ferroelectricity in orthorhombic $YFeO_3$,[12] it has still been a controversial topic.[13,14] Furthermore, there are few studies so far about the ferroelectric properties of orthorhombic $YFeO_3$ film, especially for the microscopic domain structures.

In our previous work,[15] the hexagonal $YFeO_3$ film was prepared by the sol–gel method combined with spin coating technique and its characteristics were analyzed. Here, we obtain the orthorhombic $YFeO_3$ film successfully, only by changing the lattice-matched substrate. This work is a short report on the electrical properties of the orthorhombic $YFeO_3$ thin film on $La_{0.67}Sr_{0.33}MnO_3/LaAlO_3$ substrate, where we consider the $La_{0.67}Sr_{0.33}MnO_3$ film as bottom electrode. In particular, its domain structure and polarization reversal behavior are studied.

2. Experimental details

The $La_{0.67}Sr_{0.33}MnO_3$ (LSMO) layer was successively deposited on $LaAlO_3$(111) (ALO) substrate by a pulsed laser deposition (PLD) method using a KrF excimer laser, with laser wavelength of 248 nm, laser repetition rate of 4 Hz, and

*Project supported by the National Natural Science Foundation of China (Grant No. 61471301), Natural Science Basic Research Program of Shaanxi, China (Grant No. 2017JQ5083), and PhD Research Startup Foundation of Xi'an University of Science and Technology, China (Grant No. 2017QDJ044).

†Corresponding author. E-mail: zrlan_69@163.com

© 2019 Chinese Physical Society and IOP Publishing Ltd

pulse energy density of 1.5 J/cm^2. The LSMO layer was deposited and annealed *in situ* at 1073 K in 10.0 Pa oxygen pressure. Subsequently, $YFeO_3$ (YFO) thin film was prepared by a conventional sol–gel spin-coating method. Details about the preparation of precursor solution can be found in Ref. [15]. The precursor solution was coated on LSMO/ALO by spin-coating process at 1500 rpm. The as-deposited film was dried in air at 453 K and the coating process was repeated to the desired thickness. The film was pyrolyzed at 723 K to remove organic residuals. Finally, the film was subject to annealing at 1223 K in air to improve its crystallinity.

The crystal structures were performed by x-ray diffraction (XRD, D/Max2550VB+/PC, Rigaku) with Cu $K\alpha$ radiation, and laser Raman microscope (inVia, Renishaw, England) with the exciting source of 533 nm laser. The thicknesses were characterized by a scanning electron microscope (SEM, JSM-5800, JEOL) operated at 20 keV. The surface morphology and piezoelectric response were investigated by atomic force microscope (AFM, MFP-3D-SA, Asylum Research) equipped with dual alternating current (AC) resonance tracking Piezoresponse force microscopy (DART-PFM). All the procedures were conducted under atmosphere condition at room temperature. Conductive cantilevers AC240TM with Pt-coated tips were used. The nominal spring constants were 2 N/m with a fundamental resonance frequency of the free tip-vibration of approximately 70 kHz. Detailed description of the PFM analysis is shown below. The leakage current and ferroelectric hysteresis-loop measurements were tested with ferroelectric test systems (Precision LC, Radiant Technologies Inc) at room temperature. Here, Pt electrode was used to form ohmic contacts with LSMO and YFO, respectively.

3. Results and discussions

Figures 1(a) and 1(b) present the surface topographies of LSMO and YFO deposited on $LaAlO_3$(111) substrate tested by atomic force microscope. It can be seen that the morphologies of LSMO and YFO are different, resulting from different preparation methods. Both layers exhibit preferable compactness without obvious defects. The root-mean-square (RMS) roughness for LSMO and YFO is about 2.94 nm and 1.985 nm, respectively. The grain size of LSMO is about 63 nm. Compared with LSMO, YFO layer possesses finer crystal grains and flatter surface. The ultra-fine grained structure of YFO layer owes to the good controlling on conditions during sol–gel process. Figure 1(c) shows the cross-sectional SEM image of the YFO/LSMO/ALO(111) sample. It can be seen that two distinct layers of YFO and LSMO exist. Additionally, the thicknesses of LSMO and YFO layers determined are about 130 nm and 125 nm, respectively.

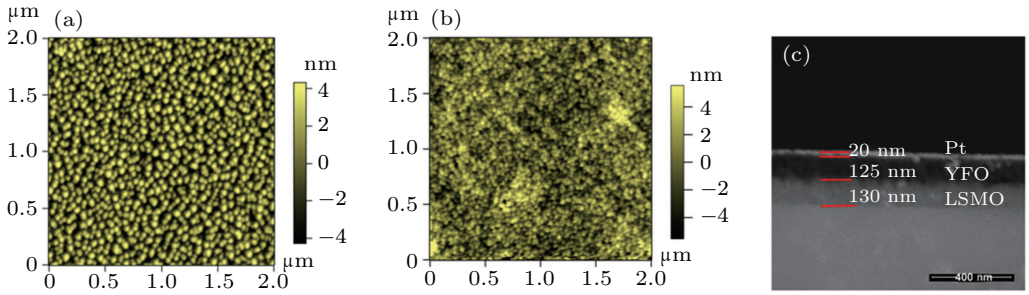


Fig. 1. (a) AFM image of the LSMO layer, (b) AFM image of the YFO layer, and (c) the cross-sectional SEM micrograph of the sample.

The XRD pattern of YFO film deposited on LSMO/LAO substrate is presented in Fig. 2(a). It reveals that XRD peaks can be disassembled to two sets of well-defined peaks, one belonging to the LSMO phase and the other belonging to the YFO phase. The diffraction peaks of LSMO phase are indexed with reference to the polycrystalline rhombohedra perovskite structure. The YFO thin film is well crystallized, with almost all of the diffraction peaks corresponding to Joint Committee on Powder Diffraction Standards (JCPDS) 39-1489. There is no diffraction of hexagonal ferrites, suggesting that the YFO thin film exists in the form of polycrystalline orthorhombic phase. It is different from the film deposited on Si substrates as discussed before.[15,16] Although the YFO film shows a different crystal structure with LSMO, but they both belong to the distortion structure of the ideal cubic perovskite ABO_3. Besides, according to the JCPDS cards of the x-ray powder diffraction patterns, the lattice constants of orthorhombic YFO ($a = 5.59$, $b = 7.61$, and $c = 5.28$) are close to the lattice constants of rhombohedra LSMO ($a = 5.53$, $b = 5.74$, and $c = 7.69$). The formation of orthorhombic perovskite structure can be attributed to the better matching possibilities between the YFO and LSMO lattices. From the viewpoint of the intensity of the diffraction peaks, both LSMO and YFO are evidently polycrystalline structure with random orientations. Besides, XRD results show that there is no diffraction peak related to prominent secondary and impurity phases (e.g. Fe_2O_3, Y_2O_3, etc).

Figure 2(b) shows the Raman spectrum of the YFO/LSMO/ALO sample. As expected, the active region for the main vibration modes of the orthoferrites is below

600 cm^{-1}, in good agreement with the already published results.[17] The vibration modes associated with the elements in "*A*" site of perovskite are located below 240 cm^{-1} for YFO. The vibration modes associated to the oxygen atoms and the octahedrons are observed between 240 cm^{-1} and 600 cm^{-1}. Compared with the results of YFO powder, a shift of the vibration modes to the left indicates an increase of the lattice parameter of YFO film, which comes from the lattice distortion induced by interfacial stress. A sharp peak positioned at 636 cm^{-1} can be ascribed to the in-plane oxygen stretching ($B_{2g}(1)$ mode) in the LSMO lattice.[18] Other characteristic peaks of LSMO, such as $A_g(2)$, $B_{3g}(4)$, and $A_g(3)$, are invisible. Note that the observed Raman signals only come from the layers of YFO and LSMO. It indicates that the penetration depth of the incited laser is lower than the thickness of the multilayer.

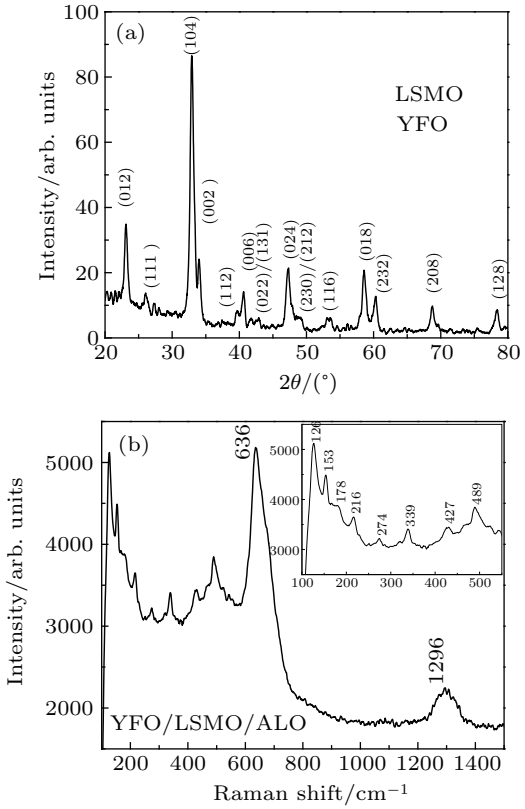


Fig. 2. (a) XRD pattern and (b) Raman spectrum of as-grown YFO/LSMO film.

Figure 3 shows the leakage current behavior and hysteresis loop of the YFO film measured from the Pt/YFO/LSMO capacitor at room temperature. The measurement configuration is displayed in the inset on the left of Fig. 3(a). We can clearly see that the experimentally observed curve is almost symmetric between negative and positive applied voltages, indicating the good conductivity of LSMO as a bottom electrode. Obviously, as the applied voltage increases, the leakage current increases. Although the leakage current density of the YFO film is lower than that of the $BiFeO_3$ film prepared by sol–gel method,[19] the value calculated about 8.39×10^{-4} A·cm^{-2} is relative large at an applied electric field of 2 V (∼ 148 kV/cm). The current density is attributed to many associated defects at the interface and oxygen vacancies. High leakage current prevents the charge carries from being preserved under high electric field. So it is difficult to get a saturated hysteresis loop at room temperature. Commonly, several conduction mechanisms are considered on the leakage behaviors in ferroelectric oxide thin films, such as the space-charge-limited current (SCLC), the Schottky emission, etc.[20] By plotting the data in various manners as a function of voltage, we find that the thermal electric conduction is the dominant mechanism for the YFO film. The inset on the right of Fig. 3(a) shows the double logarithm plots of current versus voltage dependence for the sample and its fitting curve. The slope of around 1 indicates the ohmic contact behavior between YFO with electrodes. That is to say, the leakage current could be accounted by the electron density produced by thermal excitation, while interfacial conductance is less dominant at the voltage range measured. Other conduction mechanisms are not observed in the film, probably because the applied electric field might not be sufficiently high.

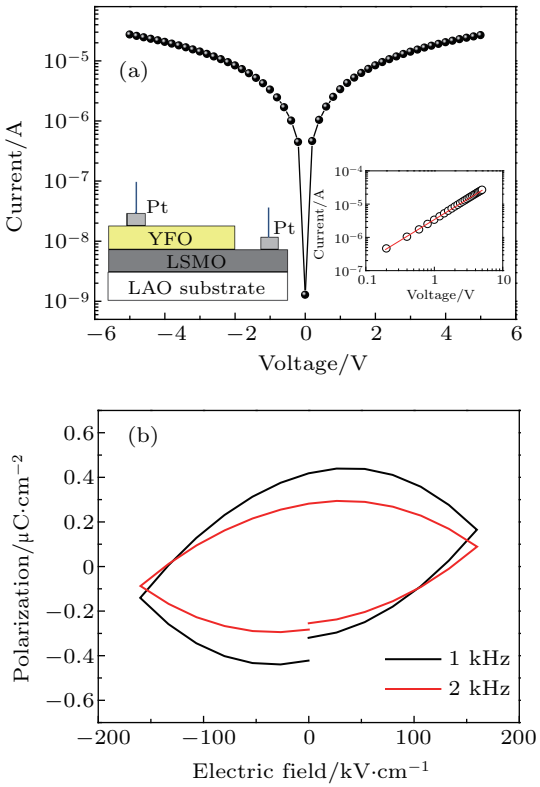


Fig. 3. (a) *I–V* characteristics of the YFO thin film on LSMO layer at room temperature; the inset on the left is the measurement chart and the inset on the right is *I–V* curve with logarithmic plots at positive bias and its fitting curve. (b) *P–E* characteristics of the YFO thin film at different frequencies.

Figure 3(b) presents the electric hysteresis loops of the YFO film at different frequencies. The *P–E* hysteresis loops exhibit ferroelectric behaviors of the YFO film with the

comparatively small polarization values comparing with the $BiFeO_3$ film.[19] We can see that the YFO film has the largest double polarization $2P_r$ of 0.5 μC/cm^2 and the coercive field E_c of 118 kV/cm at 150 kV/cm and 2 kHz. The polarization measured at 2 kHz is lower than that at 1 kHz. It reveals that the large frequency can weaken the influence of the interfacial inject charges. Note that we have used the frequency as high as possible (2 kHz) to eliminate the inject charges, which was also different with lossy dielectrics.[21] The unsaturated loops also appeared in some classical ferroelectric thin films.[22]

The nanoscopic ferroelectric characteristics of the YFO film are characterized by piezoelectric force microscopy. The capacitive layer of YFO formed between the bottom electrode of LSMO and the conducting scanning probe has been measured. Figure 4 shows the vertical piezoresponse amplitude and phase images as well as the topography image. As observed in Fig. 4(c), the dark and bright contrasts represent different polarization directions of the ferroelectric domains. Although the phase image contrast is weak, domain related response could still be detected. Due to the scanning range scale, the grain structure and morphology cannot be clearly detected. As the domain structure of thin films is related to the grain size,[23] we cannot conclude whether there is a single domain structure of grains in the YFO film.

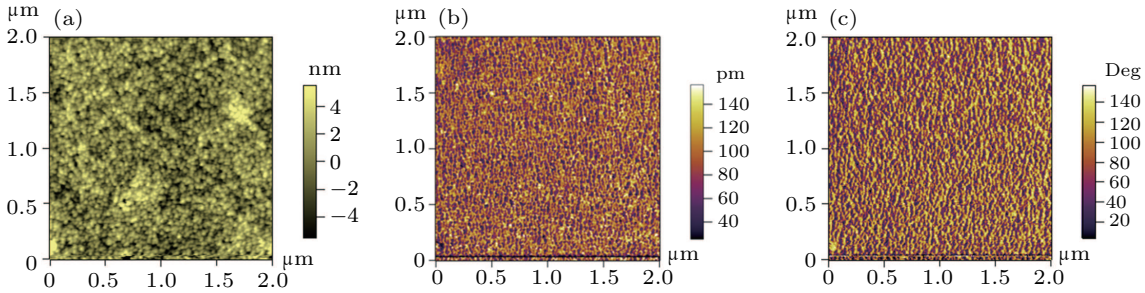


Fig. 4. PFM images of YFO film over 2 μm×2 μm: (a) topography, (b) amplitude, and (c) phase.

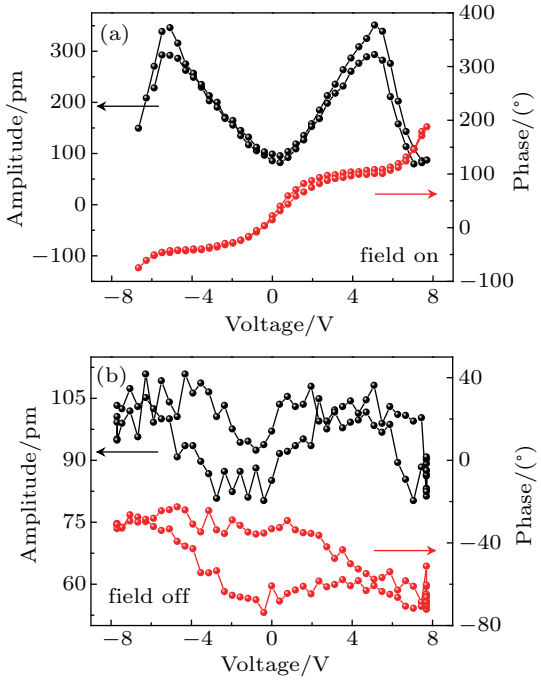


Fig. 5. PFM amplitude (black) and phase (red) loops proving the ferroelectric nature of the YFO layer sandwiched between the tip and LSMO: (a) on-field mode and (b) off-field mode.

In order to get a better insight into the local switching behavior of ferroelectric domains, piezoresponse loops are recorded by placing the tip over the center of the grains and in the on-field and off-field modes, respectively. As can be seen in Fig. 5, the butterfly-like amplitude response with the corresponding phase hysteresis has been successfully acquired in the two field modes. It provides an evidence for polarization rotation or "switching" behavior in the orthorhombic YFO thin film. Due to the asymmetry of the tip/film/bottom electrode and/or the presence of an internal electric field inside the film, there is a shift of the loops to the positive voltage. These results are in concordance with results reported before.[24] Compared with the loops in the off-field mode, the shift in the on-field mode is relatively large, indicating a higher internal electric field, which is mainly caused by the movement of oxygen vacancies under the action of the electric field.[25]

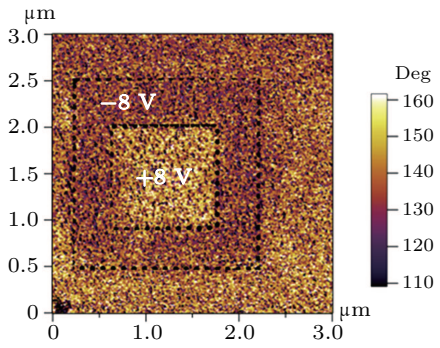


Fig. 6. DART-PFM phase image without DC voltage after the "box-in-box" writing processes.

Further, local poling experiment has been performed so as to testify successful polarization switching. The sample was poled under direct current (DC) voltages with "box-in-box" writing processes. In the "box-in-box" writing processes, −8 V was applied on a 2×2 μm^2 area, and +8 V was applied on a 1×1 μm^2 square inside simultaneously. Figure 6

shows the DART-PFM image without DC voltage after the writing processes. It can be seen that the polarizations are rotated to downward direction with the bias of -8 V (dark color) and the polarizations are rotated to upward direction with the bias of $+8$ V (bright color). Phase image contrast was quite weak. However, polarized response could still be detected. It confirms that polarization reversal is indeed possible in orthorhombic YFO film at room temperature.

4. Conclusions

In summary, $YFeO_3$ thin film with another crystal structure is prepared on LSMO/LAO substrate by a sol–gel spin-coating method. X-ray diffraction pattern and Raman spectrum reveal that the YFO film is polycrystalline orthorhombic structure. The leakage current density of the YFO film is 8.39×10^{-4} A·cm^{-2} at an applied electric field of about 148 kV/cm. Due to the large leakage current, the unsaturated *P*–*E* loop is obtained at the room temperature. PFM phase image of the YFO film reveals weak ferroelectric domain structure and its polarization can be rotated under the external field. The present work promotes the understanding of the multiferroic properties in orthorhombic YFO.

References

[1] Spaldin N A, Cheong S W and Ramesh R 2010 *Phys. Today* **63** 38
[2] Eerenstein W, Mathur N D and Scott J F 2006 *Nature* **442** 759
[3] Pyatakov A P and Zvezdin A K 2012 *Phys.-Usp.* **55** 557
[4] Udalov O G, Chtchelkatchev N M and Beloborodov I S 2014 *Phys. Rev. B* **89** 174203
[5] Raymond-Herrera O, Góngora-Lugo P, Ostos C, Curiel-Alvarez M, Bueno-Baques D, Machorro-Mejia R, Mestres-Vila L, Font-Hernández R, Portelles-Rodriguez J and Siqueiros J M 2012 *MRS Proc.* **1454** 51
[6] Maiti R, Basu S and Chakravorty D 2009 *J. Magn. Magn. Mater.* **321** 3274
[7] Tokunaga Y, Furukawa N, Sakai H, Taguchi Y, Arima T H and Tokura Y 2009 *Nat Mater.* **8** 558
[8] Tokunaga Y, Iguchi S, Arima T and Tokura Y 2008 *Phys. Rev. Lett.* **101** 097205
[9] Lee J H, Jeong Y K, Park J H, Oak M A, Jang H M, Son J Y and Scott J F 2011 *Phys. Rev. Lett.* **107** 117201
[10] Jeong Y K, Lee J H, Ahn S J, Song S W, Jang H M, Choi H and Scott J F 2012 *J. Am. Chem. Soc.* **134** 1450
[11] Mathur S, Veith M, Rapalaviciute R, Shen H, Gerardo F G, Waldir L Martins F and Thelma S B 2004 *Chem. Mater.* **16** 1906
[12] Shang M Y, Zhang C Y, Zhang T S, Yuan, Ge L, Yuan H M and Feng S H 2013 *Appl. Phys. Lett.* **102** 062903
[13] Zhang R L, Chen C L, Jin K X, Niu L W, Xing H and Luo B C 2014 *J. Electroceram* **32** 187
[14] Ma Y, Chen X M and Lin Y Q 2008 *J. Appl. Phys.* **103** 124111
[15] Zhang R L, Chen C L, Zhang Y J, Xing H, Dong X L and Jin K X 2015 *Chin. Phys. B* **24** 017701
[16] Zhang R L, Xiong S X, Gong M, Wang X Q, Yu C X and Lan J P 2018 *J. Electroceram.* **40** 156
[17] Coutinho P V, Cunha F and Barrozo P 2017 *Solid State Commun.* **252** 59
[18] Chen C Z, Li Y and Wang B 2013 *Solid State Commun.* **161** 1
[19] Liu Z L, Liu H R, Du G H, Zhang J and Yao K L 2006 *J. Appl. Phys.* **100** 044110
[20] Juan P C, Chen S M and Lee J Y 2004 *J. Appl. Phys.* **95** 3120
[21] Scott J F 2008 *J. Phys.: Condens. Matter* **20** 021001
[22] Murtaza T, Salmani I A, Ali J and Khan M S 2018 *J. Mater. Sci.: Mater. Electron.* **29** 5110
[23] Ren S B, Lu C J, Liu J S, Shen H M and Wang Y N 1996 *Phys. Rev. B* **54** R14337
[24] Xiao J, Herng T S, Ding J and Zeng K 2017 *J. Alloy Compd.* **709** 535
[25] Jesse S, Baddorf A P and Kalinin S V 2006 *Appl. Phys. Lett.* **88** 062908